

Magnetization and Intrinsic Coercivity for τ -phase $\text{Mn}_{54}\text{Al}_{46}$ / α -phase $\text{Fe}_{65}\text{Co}_{35}$ Composite

Jihoon Park¹, Yang-Ki Hong^{1*}, Jaejin Lee¹, Woncheol Lee¹, Chul-Jin Choi², Xia Xu³, and Alan M. Lane³

¹Department of Electrical and Computer Engineering and MINT Center, the University of Alabama, Tuscaloosa, Alabama 35487

²Korea Institute of Materials Science, Changwon, Kyungsangnam-do, Republic of Korea (South Korea)

³Department of Chemical and Biological Engineering and MINT Center, the University of Alabama, Tuscaloosa, Alabama 35487

(Received 4 November 2013, Received in final form 2 March 2014, Accepted 3 March 2014)

We have synthesized ferromagnetic τ -phase $\text{Mn}_{54}\text{Al}_{46}$ / α -phase $\text{Fe}_{65}\text{Co}_{35}$ composite by annealing a mixture of paramagnetic ε -phase $\text{Mn}_{54}\text{Al}_{46}$ and ferromagnetic α -phase $\text{Fe}_{65}\text{Co}_{35}$ particles at 650 °C. The volume fraction (f_h) of hard τ -phase $\text{Mn}_{54}\text{Al}_{46}$ of the composite was varied from 0 to 1. During the annealing, magnetic phase transformation occurred from paramagnetic ε -phase to ferromagnetic τ -phase $\text{Mn}_{54}\text{Al}_{46}$. The magnetization and coercivity of the composite monotonically decreased and increased, respectively, as the f_h increased. These results are in good agreement with our proposed composition dependent coercivity and modified magnetization equations.

Keywords : permanent magnet, magnetic composites, exchange coupling, Mn-Al, Fe-Co

1. Introduction

A figure of merit for permanent magnets is the maximum energy product $(BH)_{\max}$. The $(BH)_{\max}$ for $\text{Nd}_2\text{Fe}_{14}\text{B}$ are theoretically 64 MGOe [1] and experimentally 56 MGOe [2]. However, a low operation temperature and limited availability of rare-earth (RE) elements are potential barriers against the use of these RE element-based permanent magnets. Therefore, discovery of RE-free permanent magnets with high $(BH)_{\max}$ is an emerging issue to address. Accordingly, ferromagnetic τ -phase Mn-Al [3, 4] receives much attention, because of its high magnetic moment ($2.4 \mu_B/\text{f.u.}$) [5, 6] and magnetocrystalline anisotropy constant ($1.5 \times 10^6 \text{ J/m}^3$) [5, 6], and low cost. It has been reported [7] that experimental remanent magnetic flux density (B_r), intrinsic coercivity (H_{ci}), and $(BH)_{\max}$ of τ -phase Mn-Al magnet are 7 kG, 2.35 kOe, and 9.2 MGOe, respectively. It is noted that those B_r , H_{ci} , and $(BH)_{\max}$ are still much lower compared to RE-based permanent magnets.

Therefore, magnetic exchange coupling between hard and soft magnetic phases has been proposed and experimentally studied to further increase $(BH)_{\max}$ of RE-free permanent magnets. Soft magnetic phase can be exchange

coupled with hard magnetic phase within two times of domain wall thickness ($2\delta_w$) of hard magnetic phase [8]. The exchange coupling makes full use of high coercivity from hard phase and magnetization from soft phase. Therefore, it is possible to achieve large $(BH)_{\max}$ of the RE-free permanent magnet by the exchange coupling. Exchange coupled magnets based on hard magnetic phases of Fe-Pt [9-11], Sm-Co [12], and $\text{Nd}_2\text{Fe}_{14}\text{B}$ [13], have been extensively studied. However, these exchange coupled magnets still contain RE or precious elements, and the exchange coupling effect is not noticeable in $\text{Nd}_2\text{Fe}_{14}\text{B}$ because there is already a high magnetic moment.

In this paper, we report a unique annealing process synthesizing two-phase hard τ -phase $\text{Mn}_{54}\text{Al}_{46}$ /soft α -phase $\text{Fe}_{65}\text{Co}_{35}$ composite magnets, and propose a simple composition dependent coercivity equation to explain experimental coercivity.

2. Experiments

Paramagnetic ε -phase $\text{Mn}_{54}\text{Al}_{46}$ particles were synthesized by gas-atomization. After having dissolved Fe- and Co-salts and dispersed the ε -phase $\text{Mn}_{54}\text{Al}_{46}$ particles in de-ionized water, a NaBH_4 solution was added to the solution. Thereby, Fe- and Co-salts were reduced to α -phase $\text{Fe}_{65}\text{Co}_{35}$ metal alloy particles. Then, ε -phase $\text{Mn}_{54}\text{Al}_{46}$ / α -phase $\text{Fe}_{65}\text{Co}_{35}$ cakes ($0 < f_h < 1$) were dried

©The Korean Magnetism Society. All rights reserved.

*Corresponding author: Tel: +1-205-348-7268

Fax: +1-205-348-6959, e-mail: ykhong@eng.ua.edu

at 100 °C, and consequently, annealed at 650 °C for 1 hour under Ar environment. The f_h is the volume fraction of magnetically hard phase. Both α -phase $\text{Fe}_{65}\text{Co}_{35}$ ($f_h = 0$) and τ -phase $\text{Mn}_{54}\text{Al}_{46}$ ($f_h = 1$) particles were also prepared as reference materials.

The crystalline phases of the $\text{Fe}_{65}\text{Co}_{35}$ and $\text{Mn}_{54}\text{Al}_{46}$ particles and their composites were identified with X-ray diffraction (XRD). A vibrating sample magnetometer (VSM) was used to characterize their magnetic properties. The particle size and size distribution were determined using transmission electron microscopy (TEM) and scanning electron microscope (SEM). Also, we have performed elemental mappings on the composites with scanning electron microscopy-energy dispersive X-ray spectrometry (SEM-EDS) to observe elemental distribution.

3. Results and Discussion

The gas-atomized $\text{Mn}_{54}\text{Al}_{46}$ is paramagnetic ε -phase, and its shape is spherical (7-70 μm in diameter), while the as-synthesized $\text{Fe}_{65}\text{Co}_{35}$ is ferromagnetic α -phase spherical chain (40 nm in average diameter). These were confirmed by XRD, SEM, and TEM, which are not shown in this paper. We have synthesized ε -phase $\text{Mn}_{54}\text{Al}_{46}/\alpha$ -phase $\text{Fe}_{65}\text{Co}_{35}$ composites with various volume fractions of hard phase, i.e. $f_h = 0.327, 0.500, 0.694, 0.773,$ and 0.819 . As described in the experimental section, the synthesized composite was annealed at 650 °C to convert the paramagnetic ε -phase $\text{Mn}_{54}\text{Al}_{46}$ to ferromagnetic τ -phase $\text{Mn}_{54}\text{Al}_{46}$. The prolonged annealing causes paramagnetic β - or γ -phase $\text{Mn}_{54}\text{Al}_{46}$ to nucleate. Therefore, we have optimized annealing time of one hour. Ferromagnetic α -phase $\text{Fe}_{65}\text{Co}_{35}$ ($f_h = 0.000$) and paramagnetic ε -phase $\text{Mn}_{54}\text{Al}_{46}$ ($f_h = 1.000$) particles were annealed, separately, under the same annealing conditions as those used for annealing of ε -

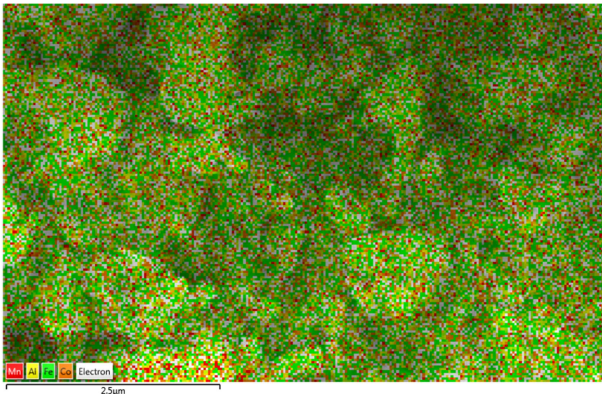


Fig. 1. (Color online) Elemental mapping image of ferromagnetic τ -phase $\text{Mn}_{54}\text{Al}_{46}/\alpha$ -phase $\text{Fe}_{65}\text{Co}_{35}$ composite ($f_h = 0.819$).

phase $\text{Mn}_{54}\text{Al}_{46}/\alpha$ -phase $\text{Fe}_{65}\text{Co}_{35}$ composites. This is because we wanted to compare magnetic properties of annealed single phase τ -phase $\text{Mn}_{54}\text{Al}_{46}$ and α -phase $\text{Fe}_{65}\text{Co}_{35}$ to those of τ -phase $\text{Mn}_{54}\text{Al}_{46}/\alpha$ -phase $\text{Fe}_{65}\text{Co}_{35}$ composite.

Figure 1 shows elemental mapping image of ferromagnetic τ -phase $\text{Mn}_{54}\text{Al}_{46}/\alpha$ -phase $\text{Fe}_{65}\text{Co}_{35}$ composite ($f_h = 0.819$). It can be seen that Mn, Al, Fe, and Co elements are well distributed, and Fe and Co elements are more concentrated on the $\text{Mn}_{54}\text{Al}_{46}$ particles' surface than Mn and Al elements. This indicates that $\text{Mn}_{54}\text{Al}_{46}$ particles are well covered with $\text{Fe}_{65}\text{Co}_{35}$ particles during the reducing and annealing processes.

Figure 2 shows XRD patterns and magnetic hysteresis loops of the τ -phase $\text{Mn}_{54}\text{Al}_{46}$, α -phase $\text{Fe}_{65}\text{Co}_{35}$, and composite with $f_h = 0.819$. All the τ -phase $\text{Mn}_{54}\text{Al}_{46}$, α -phase $\text{Fe}_{65}\text{Co}_{35}$, and composite ($f_h = 0.819$) are well crystallized. The τ -phase $\text{Mn}_{54}\text{Al}_{46}$ shows the saturation

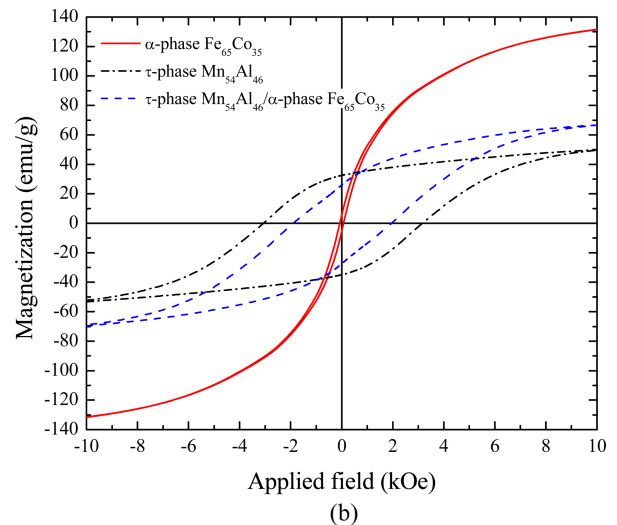
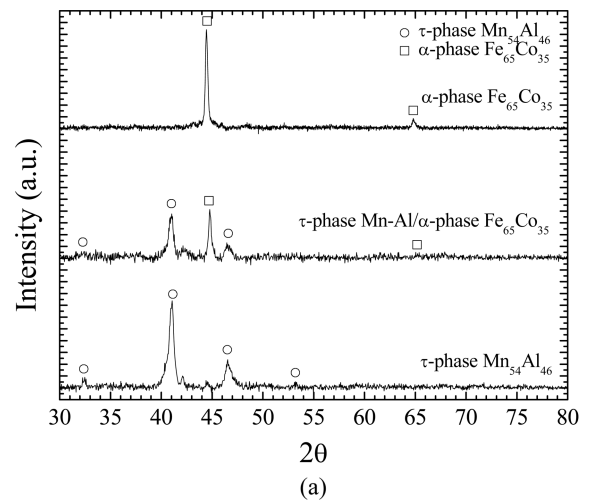


Fig. 2. (Color online) (a) the XRD patterns and (b) hysteresis loops for synthesized single phase τ -phase $\text{Mn}_{54}\text{Al}_{46}$, α -phase $\text{Fe}_{65}\text{Co}_{35}$, and composite ($f_h = 0.819$).

magnetization of 53 emu/g and intrinsic coercivity (H_{ci}) of 3093 Oe, and α -phase $\text{Fe}_{65}\text{Co}_{35}$ shows 131 emu/g and 75 Oe as shown in Fig. 2(b). It is noted that the magnetization of α -phase $\text{Fe}_{65}\text{Co}_{35}$ powder is lower than 240 emu/g of its bulk value [14]. This is due to the thermal agitation of magnetization, slight oxidation of $\text{Fe}_{65}\text{Co}_{35}$ particle or incomplete reduction of Fe- and Co-salts. After converting a mixture of paramagnetic ε -phase $\text{Mn}_{54}\text{Al}_{46}$ and ferromagnetic α -phase $\text{Fe}_{65}\text{Co}_{35}$ particles to ferromagnetic τ -phase $\text{Mn}_{54}\text{Al}_{46}$ /soft α -phase $\text{Fe}_{65}\text{Co}_{35}$ composite ($f_h = 0.819$), the saturation magnetization increased to 69 emu/g from 53 emu/g in Fig. 2(b). On the other hand, the H_{ci} decreased to 1926 Oe from 3093 Oe. No kink was observed from hysteresis loops of τ -phase $\text{Mn}_{54}\text{Al}_{46}$ / α -phase $\text{Fe}_{65}\text{Co}_{35}$ composites with $0 \leq f_h \leq 1$. However, the remanent magnetization of the composite was lower than that of the hard phase. The exchange coupling between hard and soft phases occurs only if the thickness of soft phase is thinner than two times of the hard phase's domain wall thickness ($2\delta_w$) [8]. The experimental δ_w of Mn-Al is 15 nm [15]. The diameter of the synthesized α -phase $\text{Fe}_{65}\text{Co}_{35}$ particle is 40 nm in average, which is greater than $2\delta_w$ (30 nm) of τ -phase $\text{Mn}_{54}\text{Al}_{46}$. Therefore, it can be assumed that the soft α -phase $\text{Fe}_{65}\text{Co}_{35}$ particles are partially involved in exchange coupling.

Figure 3(a) and (b) show f_h dependence of magnetization $\sigma(f_h)$ and intrinsic coercivity $H_{ci}(f_h)$ for ferromagnetic τ -phase $\text{Mn}_{54}\text{Al}_{46}$ / α -phase $\text{Fe}_{65}\text{Co}_{35}$ composites. The magnetization monotonically decreases as the f_h increases, while the intrinsic coercivity increases. We now analyze $\sigma(f_h)$ and $H_{ci}(f_h)$ for ferromagnetic τ -phase $\text{Mn}_{54}\text{Al}_{46}$ / α -phase $\text{Fe}_{65}\text{Co}_{35}$ composites. According to theoretical studies on two-phase composite magnet, the saturation magnetization [8] and anisotropy constant [16] of composite can be expressed as:

$$\sigma = \frac{\sigma_h \rho_h f_h + \sigma_s \rho_s f_s}{\rho_h f_h + \rho_s f_s} \quad (1)$$

$$K = (1 - f_h)K_s + f_h K_h, \quad (2)$$

where σ is the saturation magnetization, K is the magnetocrystalline anisotropy constant, and ρ is the density. h and s in the subscript denote hard and soft phase, respectively. Because of the experimental difficulty of obtaining K , we have developed an expression for H_{ci} of two-phase magnetic composite using experimentally accessible H_{ci} for both hard and soft phases. H_{ci} due to magnetocrystalline anisotropy [17] is

$$H_{ci} = \frac{\alpha K}{\sigma \rho}, \quad (3)$$

where α is a constant depending on the crystal structure

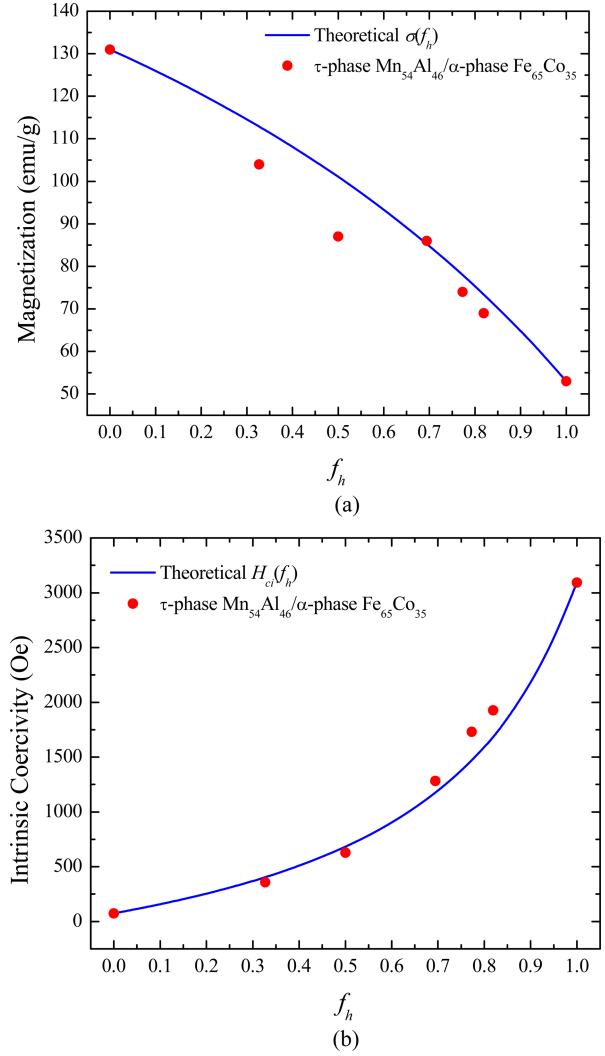


Fig. 3. (Color online) The calculated and experimental f_h dependence of (a) magnetization $\tau(f_h)$ and (b) intrinsic coercivity $H_{ci}(f_h)$ for τ -phase $\text{Mn}_{54}\text{Al}_{46}$ / α -phase $\text{Fe}_{65}\text{Co}_{35}$ composites.

and degree of alignment. For aligned particles, α is 2; for unaligned (random) particles, α is 0.64 for cubic crystals and 0.96 for uniaxial crystals. Then, H_{ci} of the two-phase magnetic composite can be modified to equation (4) by combining Eqs. (2) and (3):

$$H_{ci} = \alpha \frac{(1 - f_h)K_s + f_h K_h}{(1 - f_h)\sigma_s \rho_s + f_h \sigma_h \rho_h}. \quad (4)$$

By replacing K in Eq. (4) with H_{ci} in Eqs. (3), Eq. (4) becomes Eq. (5).

$$H_{ci} = \alpha \frac{\sigma_s \rho_s H_s (1 - f_h) + \sigma_h \rho_h H_h f_h}{\sigma_s \rho_s (1 - f_h) + \sigma_h \rho_h f_h}. \quad (5)$$

Equation (5) suggests that the coercivity of a composite

can be estimated by experimental H_{ci} of hard and soft phase materials instead of K of each material.

The σ and H_{ci} of single phase τ -phase $\text{Mn}_{54}\text{Al}_{46}$ ($\sigma_h = 53$ emu/g and $H_h = 3093$ Oe) and α -phase $\text{Fe}_{65}\text{Co}_{35}$ ($\sigma_s = 131$ emu/g and $H_s = 75$ Oe) were used as input parameters in Eqs. (1) and (5) to calculate $\sigma(f_h)$ and $H_{ci}(f_h)$. The calculated $\sigma(f_h)$ and $H_{ci}(f_h)$ are shown in Fig. 3, and are in good agreement with the experimental results. Therefore, our developed coercivity equation, i.e. Eq. (5), serves as guidance to predict H_{ci} for two-phase magnetic composite.

4. Conclusion

Ferromagnetic τ -phase $\text{Mn}_{54}\text{Al}_{46}$ ($f_h = 1.000$), α -phase $\text{Fe}_{65}\text{Co}_{35}$ ($f_h = 0.000$), and τ -phase $\text{Mn}_{54}\text{Al}_{46}$ / α -phase $\text{Fe}_{65}\text{Co}_{35}$ composites ($0 < f_h < 1$) were synthesized. The magnetization and intrinsic coercivity of single phase τ -phase $\text{Mn}_{54}\text{Al}_{46}$ were 53 emu/g and 3090 Oe, and those of single phase α -phase $\text{Fe}_{65}\text{Co}_{35}$ were 131 emu/g and 75 Oe, respectively. The magnetization and intrinsic coercivity of two-phase magnetic composite monotonically decreased and increased, respectively, as the f_h increased.

The experimental intrinsic coercivity and magnetization of the composite with various f_h are in good agreement with the proposed coercivity and modified magnetization equations, respectively.

References

- [1] M. Sagawa, S. Fujimara, H. Yamamoto, Y. Matsuura, and S. Hirosawa, *J. Appl. Phys.* **57**, 4094 (1985).
- [2] S. Sugimoto, *J. Phys. D: Appl. Phys.* **44**, 064001 (2011).
- [3] H. Kono, *J. Phys. Soc. Jpn.* **13**, 1444 (1958).
- [4] A. J. J. Koch, P. Hokkelling, M. G. V. D. Steeg, and K. J. DeVos, *J. Appl. Phys.* **31**, S75 (1960).
- [5] A. Sakuma, *J. Phys. Soc. Jpn.* **63**, 1422 (1993).
- [6] J. H. Park, Y. K. Hong, S. Bae, J. J. Lee, J. Jalli, G. S. Abo, N. Neveu, S. G. Kim, C. J. Choi, and J. G. Lee, *J. Appl. Phys.* **107**, 09A731 (2010).
- [7] T. Kubo, US Patent 3,976,519 (1976).
- [8] E. F. Kneller and R. Hawig, *IEEE Trans. Magn.* **27**, 3588 (1991).
- [9] Y. Liu, A. George, R. Skomski, and D. J. Sellmyer, *Appl. Phys. Lett.* **99**, 172504 (2011).
- [10] H. Zeng, S. Sun, J. Li, Z. L. Wang, and J. P. Liu, *Appl. Phys. Lett.* **85**, 792 (2004).
- [11] B. Ma, H. Wang, H. Zhao, C. Sun, R. Acharya, and J. P. Wang, *J. Appl. Phys.* **109**, 083907 (2011).
- [12] M. Marinescu, J. F. Liu, M. J. Bonder, and G. C. Hadjipanayis, *J. Appl. Phys.* **103**, 07E120 (2008).
- [13] C. W. Kim, Y. H. Kim, H. G. Cha, J. C. Kim, and Y. S. Kang, *Mol. Cryst. Liq. Cryst.* **472**, 155 (2007).
- [14] C. W. Chen, *J. Appl. Phys.* **32**, S348 (1961).
- [15] G. F. Korznikova, *J. Microsc.* **239**, 239 (2010).
- [16] R. Skomski and J. M. D. Coey, *Phys. Rev. B* **48**, 15812 (1993).
- [17] C. Kittel, *Rev. Mod. Phys.* **21**, 541 (1949).